

Design method of reusable reciprocal invisibility and phantom device

Cheng-Fu Yang(杨成福), Li-Jun Yun(云利军), and Jun-Wei Li(李俊玮)

Citation: Chin. Phys. B, 2022, 31 (**8**): 084101. DOI: 10.1088/1674-1056/ac6166
Journal homepage: http://cpb.iphy.ac.cn; http://iopscience.iop.org/cpb

What follows is a list of articles you may be interested in

Reflectionless spatial beam benders with arbitrary bending angle by introducing optic-null medium into transformation optics

Fei Sun(孙非), Yi-Chao Liu(刘一超), Yi-Biao Yang(杨毅彪), Hong-Ming Fei(费宏明), Zhi-Hui Chen(陈智辉), and Sai-Ling He(何赛灵)

Chin. Phys. B, 2021, 30 (**3**): 034101. DOI: 10.1088/1674-1056/abd38b

Homogeneous transparent device and its layered realization

Cheng-Fu Yang(杨成福), Ming Huang(黄铭), Jing-Jing Yang(杨晶晶), Fu-Chun Mao(毛福春), Ting-Hua Li(李廷华), Peng Li(黎鹏), Peng-Shan Ren(任鹏姗)

Chin. Phys. B, 2018, 27 (**12**): 124101. DOI: 10.1088/1674-1056/27/12/124101

Optimization of loss and gain multilayers for reducing the scattering of a perfect conducting cylinder

Zhen-Zhong Yu(余振中), Guo-Shu Zhao(赵国树), Gang Sun(孙罡), Hai-Fei Si(司海飞), Zhong Yang(杨忠)

Chin. Phys. B, 2016, 25 (**7**): 074101. DOI: 10.1088/1674-1056/25/7/074101

Design of two-dimensional elliptically cylindrical invisible cloaks with multiple regions

Luo Xiao-Yang, Liu Dao-Ya, Liu Jin-Jing, Dong Jian-Feng

Chin. Phys. B, 2014, 23 (**5**): 054101. DOI: 10.1088/1674-1056/23/5/054101

Manipulating surface plasmon waves by transformation optics: Design examples of beam squeezer, bend, and omnidirectional absorber

Yu Zhen-Zhong, Feng Yi-Jun, Wang Zheng-Bin, Zhao Jun-Ming, Jiang Tian

Chin. Phys. B, 2013, 22 (**3**): 034102. DOI: 10.1088/1674-1056/22/3/034102

Design method of reusable reciprocal invisibility and phantom device

Cheng-Fu Yang(杨成福)[†], Li-Jun Yun(云利军)[‡], and Jun-Wei Li(李俊玮)

School of Information Science and Engineering, Yunnan Normal University, Kunming 650500, *China*

(Received 25 January 2022; revised manuscript received 22 March 2022; accepted manuscript online 28 March 2022)

Reusable reciprocal invisibility and phantom device is proposed and designed based on multi-folded transformation optics and equivalent components. In comparison with the reported reciprocal invisibility cloaks, the material parameters of the device presented here are homogeneous, and the hiding of the target object does not require any "anti-object" at all, which dramatically breaks through the limitations of the "anti-object" design in previous reciprocal cloak design. Perfectly illusion effect is also found by reasonably setting the material parameters of the restored medium of the device, which can be used to confuse detection radars while hiding target objects. Last but not least, the proposed device has an open structure, which enables the target object enclosed by the device to perform material exchange and simplex transfer of information with the outside world through open channels. In other words, the proposed device has a reusable function, enabling stealth or phantom of new target objects without changing any parameters of the device.

Keywords: transformation optics, reciprocal cloak, illusion, invisibility

PACS: 41.20.Jb, 78.20.Bh, 78.67.Pt **DOI:** 10.1088/1674-1056/ac6166

1. Introduction

Invisibility is one of the most desired skills of human beings. The traditional invisibility technology is mainly to attache the absorbing material to the surface of the object, or designs the object into a special geometric structure to weaken the reflected electromagnetic wave, thereby reducing the amount of information captured by the detection radar to achieve the purpose of stealth. It is widely used in stealth fighter jets and other military fields. However, this stealth technology is difficult to achieve the ideal stealth effect. Fortunately, the rise of metamaterials[1–3] and transformation optics[4–6] has provided a new invisibility mechanism by designing metamaterials with special electromagnetic intrinsic parameter distributions calculated by coordinate transformation method to guide and control the traveling direction of electromagnetic wave, thereby realizing the purpose of invisibility or illusion. The successive achievements of invisibility cloak experiments[7–11] in different frequency bands promote the development of this new invisible phantom technology. Furthermore, this invisible phantom technology has also been extended to other physical fields.[12–15]

Invisibility technologies based on metamaterials and transformation optics can be roughly grouped into four categories: double-blind stealth, interactive stealth, phantom stealth, and stealth carpet. The double-blind stealth technology can make the incident electromagnetic waves perfectly bypass the middle stealthy area of the cloak[4,16–18] to achieve an ideal invisibility effect, but since the incident electromagnetic waves cannot penetrate through the enclosed area of the cloak, the detector and the stealthy object are isolated from each other and cannot communicate mutually. Interactive stealth technology uses complementary media to place the target object outside the invisibility cloak,[19–23] and the object can actively perceive the external incident detection signal without being detected. The disadvantage of this technology is that for a specific stealthy object, a unique anti-object needs to be configured according to its position and material information, so as to achieve strict optical cancellation between the object and the anti-object.[19,20,24] This one-to-one correspondence determines that the position and size of the stealthy object cannot be changed at will. Phantom invisibility technology maps one target object into another object through transformation optics method to achieve the effect of confusing and indirect invisibility.[25–31] Usually the stealthy target objects are placed inside the device. Although simplex communication can be achieved, the stealthy target objects are difficult to replace, and the reusability of phantom devices is low. It should be noted that the invisible cloaks designed by the aforementioned three technologies are mainly obtained based on the transformation optics method proposed by Pendry,[4] which is established under the condition of wave optics. The characteristics of the cloaks based on this transformation method are that the electromagnetic parameters of the material are derived from the formal invariance of Maxwell's equations before and after being tranformed, and the material parameters often show strong anisotropy, which is not conducive to experiments. However, they are essentially all-space stealth technologies, which are stealthy in the true sense and still have important research values. Unlike the previous methods, stealth carpet technology is based on the quasi-conformal transformation optics approach,[32] which is valid in both wave and

[†]Corresponding author. E-mail: 421893551@qq.com
[‡]Corresponding author. E-mail: yunlijun@ynnu.edu.cn

© 2022 Chinese Physical Society and IOP Publishing Ltd

geometrical optics. An outstanding advantage of this method is that it can significantly eliminate the anisotropy of material parameters, thus facilitating experimental confirmation of the invisibility cloak.[8–11] However, this technique belongs to half-space cloaking, it only makes a curved ground look like a flat ground to the outside world.[32,33] In other words, the object placed under the carpet cloak is mapped into a flat surface, rather than disappearing from the transmitted electromagnetic waves, so this carpet stealth technology is not truly invisible.

By using the idea of complementary medium, Han *et al.* have designed a double-blind invisibility cloak with an open structure[34] or a distributed structure,[35] which can conveniently build the connection between the target object and the outside world. Similarly, remote interaction invisibility cloak with open structures has been proposed by Zheng *et al.*[36] and Chen *et al.*,[37] which can be used to hide any target object. The advantages of these stealthy devices are that the target object can be replaced conveniently, which is beneficial to reusing the stealth device. However, since these devices are local improvements made on the shell of the traditional double-blind invisibility cloak device, they cannot really resolve the communication problem between the target stealthy object and the outside world. As early as 2011, we proposed a reciprocal invisibility cloak,[38] which can make the target object inside unable to be detected by external equipment while maintaining simplex communication with the outside world. Like the external invisibility cloak, the reciprocal cloak is essentially an interactive cloak. Several reciprocal cloaks have been proposed in the past few years, including two-dimensional (2D) and three-dimensional (3D) devices.[39–41] However, all of these devices have a closed geometry each, and the target object inside the device is difficult to replace. Furthermore, objects to be cloaked inside still need to place anti-objects inside the device, that is, the stealth ability of the device is closely related to the location and size of the object to be cloaked. In order to solve these problems, the open design idea is integrated into the design of reciprocal stealth and illusion device to achieve the function of reuse. In addition, it is interesting that the device does not need equipping with a corresponding anti-object to hide the target object. The effectiveness and performance of the device are simulated and verified by finite element simulation software. The highlight of this device is that the object to be invisible or hallucinated can perform simplex communication with the outside world, and it can be flexibly replaced through an open channel. This performance makes the device promising for applications in the defense and military fields.

2. Theoretical model

The key to the method of designing the reusable interactive stealth phantom device is the equivalent component as shown in Fig. 1. According to the idea of folding geometric transformation and complementary media, the outermost ring layer ($b < r < c$) (the free space) in Fig. 1(a) is folded into the black ring layer ($a < r < b$) in the middle, forming the complementary medium region. Optical cancellation can be realized between complementary medium region and the free space region. In order to restore the influence of spatial optical cancellation on the wavefront and phase of electromagnetic waves, it is necessary to compress the entire transformed space into the green region ($r < a$) in the middle to form a restored medium layer. After the aforementioned two transformation steps of folding and compressing, the entire transformation space ($r < c$) is visually consistent with the equivalent component composed of complementary medium region (black region) and restored medium region (green region). Since the green area is obtained by compressive transformation, when a red object with material parameters of ε_o'' and μ_o'' is embedded into the green area shown in Fig. 1(b), the size of its equivalent object in the virtual space will become larger as indicated by the red object with material parameters of ε_o and μ_o in Fig. 1(c). In other words, an object with larger size in the virtual space shown in Fig. 1(c) can be equivalent to a smaller object embedded in the equivalent component shown in Fig. 1(b). If the red area in the virtual space shown in Fig. 1(c) happens to be the wrapping layer of the stealth or phantom device during transformation, it can be replaced by the equivalent component shown in Fig. 1(b), leaving an channel to the inside of the device around the equivalent component ($b < r < c$). By using this channel, the internal object can be replaced and the device can be reused. Therefore, solving the material parameters of equivalent components becomes the key to reusable phantom devices.

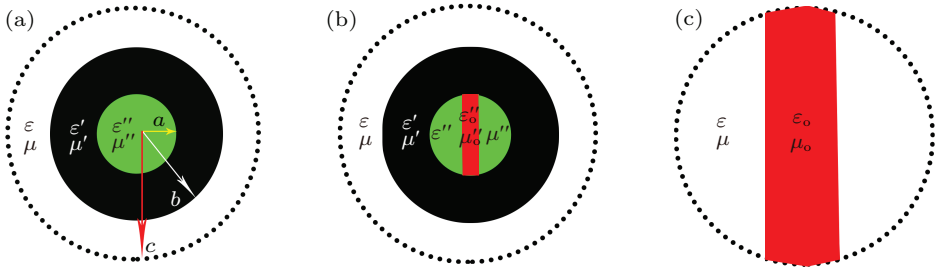


Fig. 1. Schematic diagram of equivalent component, showing (a) folding transformation process, (b) equivalent components, and (c) objects that are visually equivalent to equivalent component in panel (b).

According to the above-mentioned equivalent transformation method, a reusable invisibility and phantom devices can be achieved by embedding an equivalent component in the boundary layer of a reciprocal cloak as shown in Fig. 2, where the region in the dotted-line-sided box in Fig. 2(a) can be replaced by the equivalent component shown in Fig. 2(b), and figure 2(c) shows the enlarged display of equivalent components in Fig. 2(b). It can be observed that a circular opening channel is formed around the equivalent component in Fig. 2(b), which can be used to change the object inside the phantom device and control it remotely. In order to calculate the material parameters of each area of the equivalent component, the center of the component shown in Fig. 2(c) is assumed to be located at (x_0, y_0), and the outer radius of the invisible channel III, the complementary medium layer II, and the restored medium layers I and IV are c', b', and a' respectively. According to transformation optics, the material parameters of the complementary medium layer II can be obtained by folding the region $b' < r < c'$ into the area $a' < r < b'$, while the material parameters of the restored medium layer I and IV can be solved by compressing the region $r < c'$ into the region $r < a'$.

For the complementary medium layer shown in Fig. 2(c), the following folding transformation is introduced:

$$r = f(r_0') = \frac{(c'-b')}{(a'-b')}(r_0'-b')+b' = k_1 r_0' + k_2, \tag{1}$$

where

$$k_1 = (c'-b')/(a'-b'), \quad k_2 = b'(a'-c')/(a'-b'),$$
$$r_0' = \sqrt{(x-x_0)^2+(y-y_0)^2}.$$

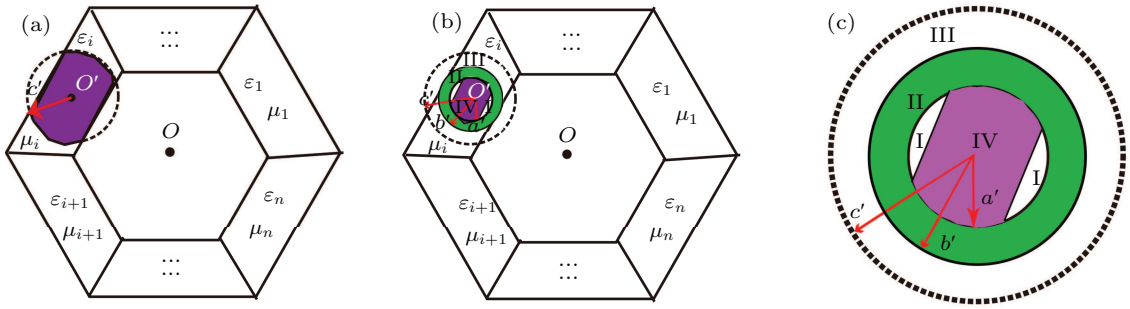


Fig. 2. Schematic diagram of reusable reciprocal invisibility and phantom device design for (a) ideal reciprocal invisibility and phantom device, (b) open-structure invisibility and phantom device containing equivalent component, and (c) enlarged display of equivalent component.

As a result, the material parameters of the complementary medium layer II are expressed as

$$\frac{\varepsilon_r}{\varepsilon} = \frac{\mu_r}{\mu} = \frac{f(r_0')}{r_0' f'(r_0')} = \frac{k_1 r_0' + k_2}{k_1 r_0'}, \tag{2a}$$
$$\frac{\varepsilon_\theta}{\varepsilon} = \frac{\mu_\theta}{\mu} = \frac{r_0' f'(r_0')}{f(r_0')} = \frac{k_1 r_0'}{k_1 r_0' + k_2}, \tag{2b}$$
$$\frac{\varepsilon_z}{\varepsilon} = \frac{\mu_z}{\mu} = \frac{f'(r_0') f(r_0')}{r_0'} = \frac{k_1(k_1 r_0' + k_2)}{r_0'}. \tag{2c}$$

Particularly, when $c' = b'^2/a'$, introducing the following folding transformation to replace Eq. (1):

$$r = f(r_0') = \frac{b'^2}{r_0'}. \tag{3}$$

And then, the material parameters of the complementary medium layer becomes

$$\frac{\varepsilon_r}{\varepsilon} = \frac{\mu_r}{\mu} = \frac{f(r_0')}{r_0' f'(r_0')} = -1, \tag{4a}$$
$$\frac{\varepsilon_\theta}{\varepsilon} = \frac{\mu_\theta}{\mu} = \frac{r_0' f'(r_0')}{f(r_0')} = -1, \tag{4b}$$
$$\frac{\varepsilon_z}{\varepsilon} = \frac{\mu_z}{\mu} = \frac{f'(r_0') f(r_0')}{r_0'} = -\frac{b'^4}{r_0'^4}. \tag{4c}$$

For the restored medium layer, the following coordinate transformation is introduced:

$$r'' = \frac{a'}{c'}|r - r_0|, \tag{5a}$$
$$\theta'' = \theta, \tag{5b}$$
$$z'' = z, \tag{5c}$$

where $r_0 = \sqrt{x_0^2 + y_0^2}$ and $r = \sqrt{x^2+y^2}$.

Equation (5) can be expressed in the rectangular coordinate system as

$$x'' = \frac{a'}{c'}(x - x_0), \tag{6a}$$
$$y'' = \frac{a'}{c'}(y - y_0), \tag{6b}$$
$$z'' = z. \tag{6c}$$

And the corresponding Jacobian matrix becomes

$$\boldsymbol{A} = \begin{bmatrix} a'/c' & 0 & 0 \\ 0 & a'/c' & 0 \\ 0 & 0 & 1 \end{bmatrix}, \tag{7}$$

Thus, the material parameters of the restored medium region I are related by

$$\frac{\varepsilon_{\mathrm{I}}''}{\varepsilon} = \frac{\mu_{\mathrm{I}}''}{\mu} = \mathrm{diag}\left[1, 1, (c'/a')^2\right]. \tag{8}$$

Since the restored medium region IV is derived from the space transformation of material parameters of ε_i and μ_i, according to transformation optics, the material parameters of the restored medium region IV are

$$\varepsilon''_{\mathrm{IV}} = \frac{\boldsymbol{A}\varepsilon_i\boldsymbol{A}^{\mathrm{T}}}{|\boldsymbol{A}|}, \tag{9a}$$

$$\mu''_{\mathrm{IV}} = \frac{\boldsymbol{A}\mu_i\boldsymbol{A}^{\mathrm{T}}}{|\boldsymbol{A}|}. \tag{9b}$$

Therefore, once the material parameters of the reciprocal invisibility and phantom device are known, an open structure can be designed according to the above mentioned method and the material parameters of equivalent components can be calculated from Eqs. (4), (8), and (9). And then, a reusable reciprocal stealth and phantom device is realized.

It should be noted that when a linear transformation method is used to design the device, the material parameters of the reusable reciprocal stealth and phantom device become homogeneous, including the complementary medium and the restore medium. Taking 2D transformation for example and introducing the following linear transformation:

$$\begin{bmatrix} x' \\ y' \\ z' \end{bmatrix} = \underbrace{\begin{bmatrix} a & b & 0 \\ c & d & 0 \\ 0 & 0 & 1 \end{bmatrix}}_{\boldsymbol{\Lambda}_i} \begin{bmatrix} x \\ y \\ z \end{bmatrix} + \begin{bmatrix} e \\ f \\ 0 \end{bmatrix}, \tag{10}$$

where e and f are the non-homogeneous terms of linear Eq. (10), and $\boldsymbol{\Lambda}_i$ is the Jacobian matrix governed by the following formula:

$$\boldsymbol{\Lambda}_i = \begin{bmatrix} a & b & 0 \\ c & d & 0 \\ 0 & 0 & 1 \end{bmatrix} = \begin{bmatrix} x'_3 - x'_1 & x'_2 - x'_1 & 0 \\ y'_3 - y'_1 & y'_2 - y'_1 & 0 \\ 0 & 0 & 1 \end{bmatrix} \times \begin{bmatrix} x_3 - x_1 & x_2 - x_1 & 0 \\ y_3 - y_1 & y_2 - y_1 & 0 \\ 0 & 0 & 1 \end{bmatrix}^{-1}, \tag{11}$$

where (x_i, y_i) and (x'_i, y'_i) indicate the coordinates before and after being transformed respectively, and 1, 2, 3 refer to the vertex order of the triangles.

According to transformation optics, the relationship among the material parameters in the regions before and after being transformed are expressed as

$$\frac{\varepsilon'_i}{\varepsilon_i} = \frac{\mu'_i}{\mu_i} = \frac{\boldsymbol{\Lambda}_i\boldsymbol{\Lambda}_i^{\mathrm{T}}}{|\boldsymbol{\Lambda}_i|}. \tag{12}$$

Since the constitutive parameter of the transformation medium described in Eq. (12) is determined only by the Jacobian matrix $\boldsymbol{\Lambda}_i$, which is only related to the coordinates of the mapped triangle vertices, the obtained constitutive parameters must be a homogenized tensor. The reciprocal invisibility and phantom device designed in this work has the characteristics of homogenization mentioned above. The COMSOL software will be used to simulate and verify its performance, and the detailed discussion will be shown in the following section.

3. Results and discussion

3.1. Reciprocal invisibility cloak with closed-structure

Figure 3 shows a schematic diagram of the space transformation of the reciprocal invisibility device with closed-structure, in which the circumradius of each polygon with A_i, B_i, C_i, and D_i as vertices is a, b, c, and d, respectively. The design principle of reciprocal invisibility cloak device with closed-structure is to fold the region $d < r < c$ in Fig. 3(a) into the region $c < r < b$ in Fig. 3(b) to form a complementary medium layer for spatial optical cancellation, and compress the area $d < r < a$ in Fig. 3(a) into the area $b < r < a$ in Fig. 3(b) to restore the electromagnetic wavefront and phase mismatch caused by the process of cancelling. When the circumradius d is small enough, the operation of compressing the area $d < r < a$ into the area $b < r < a$ can be regarded as the design of a closed-structure invisibility cloak device, and the introduction of the complementary medium layer can allow electromagnetic waves to penetrate into the interior of the cloak, so that the internal target object has the ability to perceive external signals. The transformation process in Fig. 3 can be expressed as the triangle areas $C_iD_iD_{i+1}$ and $C_iC_{i+1}D_{i+1}$ in the virtual space, which are folded into the triangle areas$C_iB_iB_{i+1}$ and $C_iC_{i+1}B_{i+1}$ in the physical space respectively, and the triangle areas $A_iA_{i+1}D_i$ and $A_{i+1}D_iD_{i+1}$ in the virtual space are respectively mapped into the triangle areas $A_iA_{i+1}B_i$ and $A_{i+1}B_iB_{i+1}$ in the physical space. By introducing Eqs. (10)–(12), the material parameters of each region in the physical space are calculated.

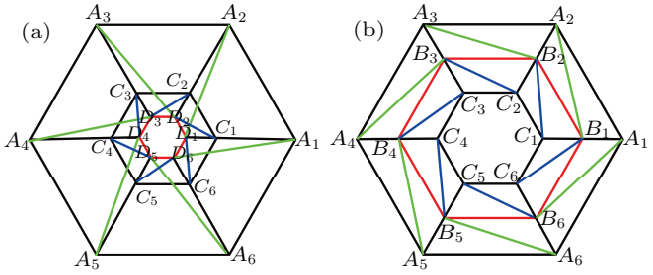


Fig. 3. Schematic diagram of spatial transformation of homogenized reciprocal invisibility cloak with closed-structure, showing (a) virtual space and (b) physical space.

Firstly, the circumradius of each polygon with A_i, B_i, C_i, and D_i as vertices is $a = 0.075$ m, $b = 0.05$ m, $c = 0.03$ m, and $d = 0.001$ m respectively, and the frequency of the incident TE electromagnetic wave is set to be 6 GHz. As a result, the calculation results of the material parameters of each region in the physical space are listed in Table 1.

Table 1. Material parameters of physical space.

Complementary medium layers									
Regions	Parameters				Regions	Parameters			
	μ_{xx}	μ_{xy}	μ_{yy}	ε_{zz}		μ_{xx}	μ_{xy}	μ_{yy}	ε_{zz}
$C_1B_1B_2$ ($C_4B_4B_5$)	−24.85	42.43	−72.5	−0.03	$C_1B_2C_2$ ($C_4B_5C_5$)	−0.38	0.44	−3.14	−1.45
$C_2B_2B_3$ ($C_5B_5B_6$)	−97.34	−0.58	−0.01	−0.03	$C_2B_3C_3$ ($C_5B_6C_6$)	−2.83	0.96	−0.69	−1.45
$C_3B_3B_4$ ($C_6B_6B_1$)	−23.84	−41.85	−73.5	−0.03	$C_2B_3C_3$ ($C_5B_6C_6$)	−2.07	−1.41	−1.45	−1.45
Restoring medium layers									
Regions	Parameters				Regions	Parameters			
	μ_{xx}	μ_{xy}	μ_{yy}	ε_{zz}		μ_{xx}	μ_{xy}	μ_{yy}	ε_{zz}
$B_1A_1A_2$ ($B_4A_4A_5$)	0.77	−1.13	2.96	2.96	$B_1A_2B_2$ ($B_4A_5B_5$)	49.67	−85.44	147.06	0.06
$B_2A_2A_3$ ($B_5A_5A_6$)	3.39	−0.38	0.33	2.96	$B_2A_3B_3$ ($B_5A_6B_6$)	196.67	0.57	0.01	0.06
$B_3A_3A_4$ ($B_6A_6A_1$)	1.43	1.51	2.30	2.96	$B_2A_3B_3$ ($B_5A_6B_6$)	48.68	84.87	148	0.06

Annotation: Owing to symmetry, the parameters of area marked with parentheses are the same as those without parentheses.

Figure 4 shows the electric field distribution of the reciprocal invisibility cloak device with the regular hexagonal polygon closed-structure, in which the core area of the cloak shown in Fig. 4(a) is a free space, and the cylindrical boundary inside the cloak shown in Fig. 4(b) is set to be the PEC boundary. For comparison, figure 4(c) shows that a cylinder with PEC boundary is placed independently in the free space. The material parameters of each triangle are shown in Table1. It can be seen that the electric field can penetrate into the reciprocal cloak, and the wavefront is perfectly restored in the front of the proposed cloak without scattering no matter whether the target object is placed inside the cloak. However, significant field scattering phenomenon can be observed when the target object is directly located in the free space. This indicates that the closed and reciprocal cloak has the ability to hide the target object as well as to sense the external signals, which is consistent with the cloaks described in the early literature.[34–37]

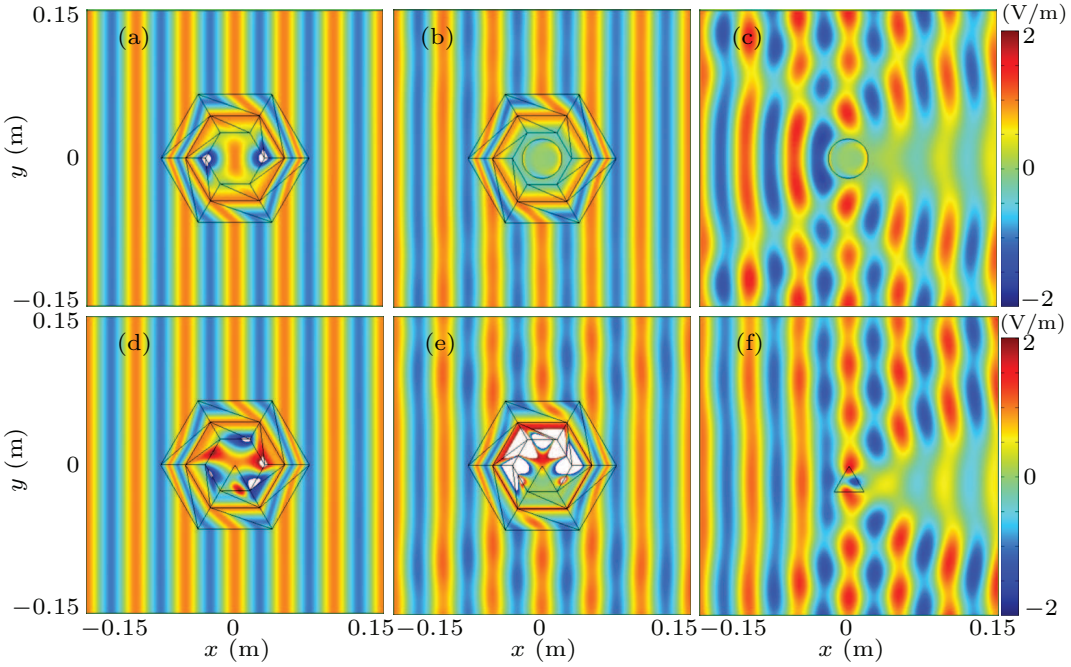


Fig. 4. Electric field distribution around (a) ideal cloak, [(b) and (c)] PEC cylinder with radius of 0.02 m, placed in the cloak or free space, [(d) and (e)] triangular object placed in cloak filled with or without "anti-object", and (f) purely triangular object in free space.

Next, the cylindrical object is replaced with a triangular-shaped object whose material parameters are $\varepsilon_0 = 6.25 + 0.01\mathrm{j}$ (the imaginary part represents the material loss) and $\mu_0 = 1$, and the "anti-object" is filled in the corresponding complementary medium region, *i.e.*, the permittivity values of the triangles $B_5A_5A_6$ and $C_5B_6C_6$ are set to be $-0.03*(6.25+0.01\mathrm{j})$ and $-1.45*(6.25+0.01\mathrm{j})$, respectively, while keeping the permeability unchanged. The near electric filed distribu-

tion is shown in Fig. 4(d). As can be seen, the triangular-shaped object becomes invisible, and the electric field can radiate to the object, *i.e.*, the target object has the capability of simplex communication, which is no different from the traditional interactive invisibility device such as the external cloak in performance. In order to investigate the characteristics of the reciprocal stealth device, the triangular-shaped object in Fig. 4(d) is kept while g the "anti-object" is removed from the complementary medium area, *i.e.*, both the permittivity and permeability of the triangle $B_5A_5A_6$ and $C_5B_6C_6$ are fixed as shown in Table 1. In such a situation, the near-electric field distribution is simulated as shown in Fig. 4(e). Figure 4(f) represents the electric field distribution when the triangular-shaped object is directly placed in the free space. From Figs. 4(d)–4(f), it can be observed that when the triangular-shaped object is directly placed in the free space, the scattering phenomenon of the electric field can be observed obviously. However, once the object is enclosed by the proposed reciprocal cloak, the scattering phenomenon nearly disappears whether the "anti-object" exists or not. Such a result shows that the invisibility capability of reciprocal stealth device with closed-structure is independent of the geometric structure nor material properties of the target object, which is the difference between the cloak designed here and the traditional interactive cloak in the early literature,[34–37] and also reflects the superiority of the cloak designed here. It should be emphasized that the size of the cloak can be enlarged if need be, but the material parameters will also change accordingly. However, in practice, owing to the use of lossy metamaterials technology to synthesize devices, factors such as the size of the metamaterial and the operating frequency of the cloak must be fully considered to satisfy the condition that the size of the metamaterial is much smaller than the wavelength. No further technical proofs are made here for brevity.

Figure 5 describes the far-field distribution of the electric field for the target object with or without the proposed reciprocal cloak. Figure 5(a) shows the far-field mode of Figs. 4(b) and 4(c), and figure 5(b) displays the far-field mode of Figs. 4(e) and 4(f). It can be observed that the far-field amplitude of the object enclosed by the cloak is well suppressed compared with the far-field amplitude of the object in the free space. The far-field amplitude drops below −24 dB and −17 dB in Figs. 5(a) and 5(b) respectively. The simulation results fully confirm the prominent stealth effect of the proposed reciprocal device.

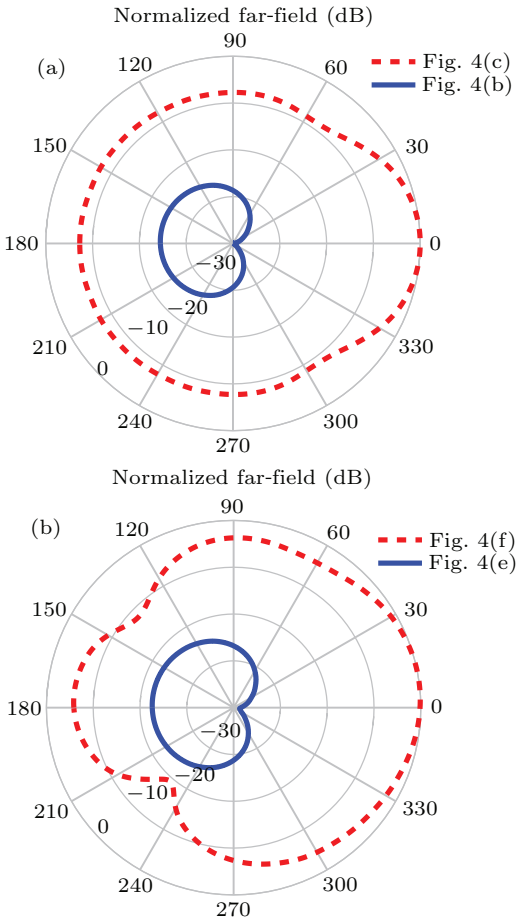


Fig. 5. Comparison between (a) far-field mode distributions of Figs. 4(b) and 4(c), and between (b) far-field mode distributions of Figs. 4(e) and 4(f).

3.2. Reusable reciprocal invisibility cloak and its performance

Next, an open channel containing cylindrical equivalent component is embedded into the reciprocal cloaking device to realize the reusable function of the device. First of all, the point of P_0 (0.04 m, 0.023 m) in the first boundary layer is taken as the center, three regions whose radii are $a' = 0.008$ m, $c' = 0.022$ m and $b' = \sqrt{a'c'} = 0.01327$ m respectively are intercepted in the above reciprocal cloaking device. According to Eq. (4), the material parameter of the complementary medium area of the equivalent component is $\varepsilon_{\rm II} = \mu_{\rm II} = \left[-1, -1, -(b'/r_0)^4\right]$, where $r_0 = \sqrt{(x-0.04)^2 + (y-0.023)^2}$. Since the equivalent region corresponding to the restored medium region IV is composed of four homogeneous and anisotropic material blocks, it is necessary to divide the region IV into four sub-regions to form a one-to-one correspondence with the blocks in the equivalent region. According to Eqs. (8) and (12), the material parameters of these four restored regions can be calculated from outside region to inside region and the results are given below.

$$\varepsilon_{\rm IV_1} = \mu_{\rm IV_1} = \begin{bmatrix} 0.77 & -1.13 & 0 \\ -1.13 & 2.96 & 0 \\ 0 & 0 & 2.96(c'/a')^2 \end{bmatrix},$$

$$\varepsilon_{\mathrm{IV}_2}=\mu_{\mathrm{IV}_2}=\begin{bmatrix}49.67 & -85.44 & 0\\ -85.44 & 147 & 0\\ 0 & 0 & 0.06(c'/a')^2\end{bmatrix},$$

$$\varepsilon_{\mathrm{IV}_3}=\mu_{\mathrm{IV}_3}=\begin{bmatrix}-24.85 & -42.44 & 0\\ 42.44 & -72.5 & 0\\ 0 & 0 & -0.029(c'/a')^2\end{bmatrix},$$

$$\varepsilon_{\mathrm{IV}_4}=\mu_{\mathrm{IV}_4}=\begin{bmatrix}-0.38 & 0.44 & 0\\ 0.44 & -3.14 & 0\\ 0 & 0 & -1.45(c'/a')^2\end{bmatrix}.$$

And the material parameter of the restored medium region I is $\varepsilon_{\mathrm{I}}=\mu_{\mathrm{I}}=\mathrm{diag}\left[1,1,(c'/a')^2\right]$.

Figures 6(a)–6(c) demonstrate the electric field distributions when a triangular-shaped object with material parameter of $\varepsilon_0=6.25+0.01\mathrm{j}$ and $\mu_0=1$ is placed at the bottom part inside the device and its corresponding "anti-object" is set in the complementary medium regions (*i.e.*, the material parameters are identical with those of Fig. 4(d)). As can be seen, no matter what the incident direction of the TE plane wave is, the open-structure reciprocal cloak has a good stealth effect. In order to study the uniqueness of the proposed device, the "anti-object" corresponding to the triangular-shaped object is removed from the complementary medium (*i.e.*, the material parameters are identical with those of Fig. 4(e)) as shown in Figs. 6(d)–6(f). It can also be found that the open-structure reciprocal cloak without "anti-object" has a good stealth effect. Comparing with the case where the "anti-object" is filled, the electric field around the device jitters slightly when no "anti-object" exists, but it does not affect the stealthy performance of the device. In addition, it should be noted that this jitter can be eliminated by further refining the calculated grids.

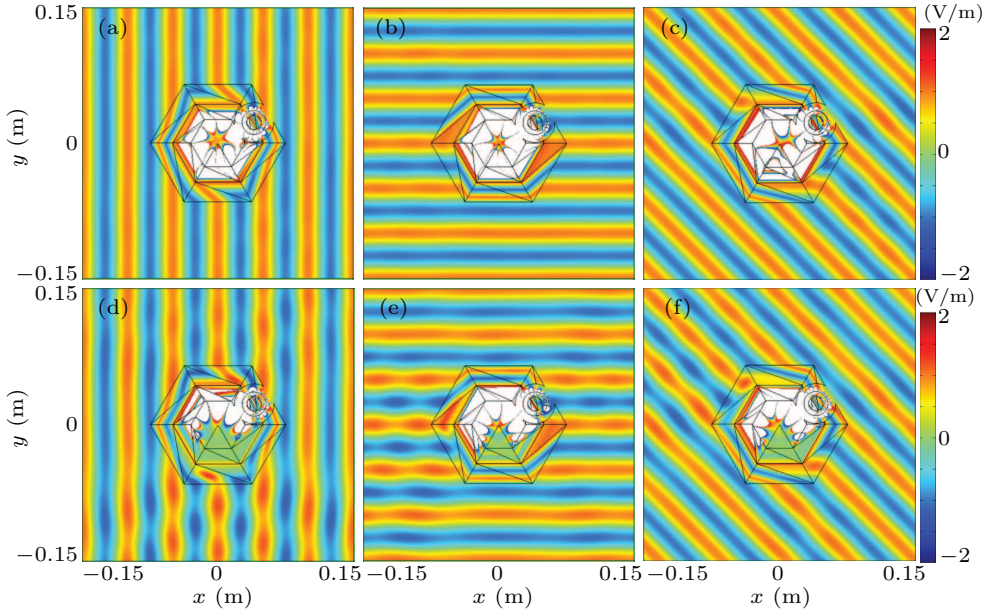


Fig. 6. Near-field distribution of electric field in open-structure reciprocal cloak, for [(a)–(c)] triangular-shaped object, which is placed at the bottom of the inner space of the device, and an "anti-object", which is filled in the complementary medium region of corresponding part of the cloak; for [(d)–(e)] triangular object, which is placed at the bottom of the inner side of the device, and the anti-object, which is removed from the corresponding complementary media layer of the cloak. The incident directions of TE plane waves are along [(a) and (d)] the X axis, [(b) and (e)] the Y axis, and oblique incident [(c) and (f)] at different angles.

The existence of the open channel makes the internal object able to be replaced easily at will, which has significant application value in reality, especially in the 3D scenes. Because in a 3D case, the target object is often enclosed by the device, and the replacement of it needs to destroy the wrapped layer of the device, which is not conducive to the device reusability. However, the function of reusability can be obtained when the device has such an open channel. To sum up, the application of open channel in the design of reciprocal stealth device not only solves the problem of simplex communication between the target object and the outside world, but also provides a reusable way of the device, which is beneficial to saving the manufacturing cost of device.

3.3. Illusion feature of reusable reciprocal cloaking device

Finally, the illusionary feature of the reusable reciprocal cloaking device is discussed. Figure 7(a) describes the near-(electric)field distribution of a triangular-shaped dielectric object with material parameters of $\varepsilon_0=6.25+0.01\mathrm{j}$ and $\mu_0=1$, and the object is placed horizontally in the free space. It should be noted that the outermost layer of the reciprocal cloak is a restored medium. According to the equivalent transformation method described in Section 2, once the material parameter of the restored medium is multiplied by ε_0 and μ_0, another large equivalent object with material parameter of ε_0 and μ_0 will be appear in the virtual space. With this mechanism, the reciprocal cloak can be turned into an illusion device as shown in

Fig. 7(b), where the triangular object in Fig. 7(a) is placed inside the open-structure reciprocal cloak also, but the restored medium of the outermost top part of the cloak are multiplied by $\varepsilon_0 = 6.25 + 0.01\mathrm{j}$ and $\mu_0 = 1$, *i.e.*, the permittivity of the triangles $C_2B_3C_3$ and $B_2A_3B_3$ are set to be $2.96 * (6.25 + 0.01\mathrm{j})$ and $0.06 * (6.25 + 0.01\mathrm{j})$ while the permeability unchanged is kept. Since the reciprocal cloak does not need the anti-object, the permittivity and permeability of the triangle $B_5A_5A_6$ and $C_5B_6C_6$ are fixed as the forth line shown in Table 1. The equivalent object with material parameters of $\varepsilon_0 = 6.25 + 0.01\mathrm{j}$ and $\mu_0 = 1$ is placed in the free space whose near-field distribution is shown in Fig. 7(c). It can be observed that the electric field distributions in Figs. 7(b) and 7(c) are identical, but they differ greatly from those in Fig. 7(a). This means that the small horizontal triangle originally placed inside the interactive cloak is visually consistent with a large inverted triangle, *i.e.*, the small triangular object is mapped into another large triangular object, and the object position is changed. Similarly, the existence of the open aisle makes it particularly easy to replace the target objects, which means that the device is reusable.

Next, the far-field distributions of the electric field corresponding to Figs. 7(a)–7(c) are calculated to quantitatively describe the illusionary function of the reusable interactive cloak as shown in Fig. 8. It can be seen that the far-field amplitude curves of Figs. 7(b) and 7(c) are almost identical, and the maximum far-field amplitude is about 1.6 V/m, and both of them are obviously different from that of Fig. 7(a). This fully demonstrates the good phantom functionality of the proposed reusable reciprocal cloak.

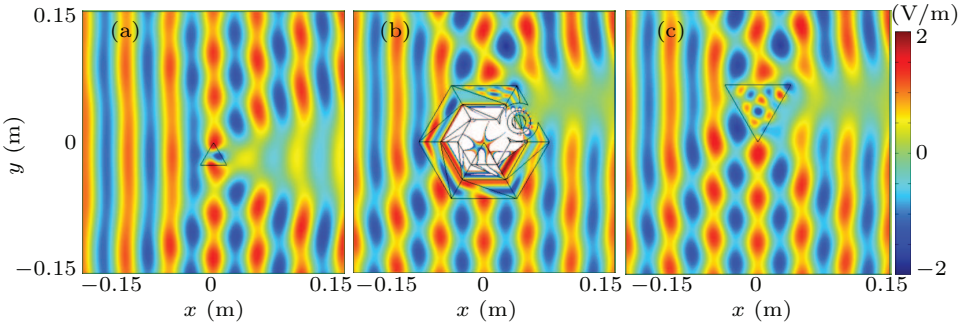


Fig. 7. Illusionary effect of reusable reciprocal cloak, indicating (a) electric field distribution of a triangular-shaped object in the free space, (b) electric field distribution of the triangular-shape object covered by the proposed reusable reciprocal cloak, and (c) electric field distribution of the equivalent object.

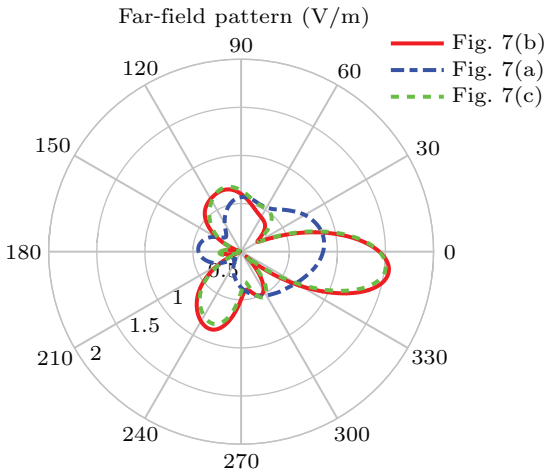


Fig. 8. Comparison among far-field modes.

4. Conclusions

In this work, based on the multi-folded transformation optics, reusable and reciprocal invisibility phantom device with homogeneous material parameters is proposed and designed. Unlike the results in previous literature, the target object to be invisible, enclosed by the proposed device, does not need using the corresponding anti-object to some extent, which removes the strict position and size dependence of object. Furthermore, by reasonably setting the parameters in the restored medium of the device, the phantom of the target object can be realized, which could be used to confuse the external detection equipment if need be. Finally, an open aisle is generated on the boundary of the closed layer of the device by introducing the equivalent component, which not only strengthens the simplex communication capability of the device, but also facilitates the replacement and remote control of the target object, so as to achieve the reusable function of the device. This helps achieve cost savings, resource reusing and intelligently controlling. It is believed that the reusable interactive invisibility phantom device presented here has the potential applications in the field of national defense and military engineering.

Acknowledgements

Project supported by the Natural Science Doctoral Research Start-Up Fund of Yunnan Normal University, China (Grant No. 01000205020503130) and the Key Project of Applied Basic Research Program of Yunnan Province, China (Grant No. 2018FA033).

References

[1] Pendry J B, Holden A J, Stewart W J and Youngs I 1996 *Phys. Rev. Lett.* **76** 4773

[2] Pendry J B, Holden A J, Robbins D J and Stewart W J 1999 *IEEE T. Microw. Theory* **47** 2075

[3] Smith D R, Padilla W J, Vier D C, Nemat-Nasser S C and Schultz S 2000 *Phys. Rev. Lett.* **84** 4184

[4] Pendry J B, Schurig D and Smith D R 2006 *Science* **312** 1780

[5] Leonhardt U 2006 *Science* **312** 1777

[6] Chen H Y, Chan C T and Sheng P 2010 *Nat. Mater.* **9** 387

[7] Schurig D, Mock J J, Justice B J, Cummer S A, Pendry J B, Starr A F and Smith D R 2006 *Science* **314** 977

[8] Liu R P, Ji C and Mock J J 2009 *Science* **323** 366

[9] Ergin T, Stenger N, Brenner P, Pendry J B and Wegener M 2010 *Science* **328** 337

[10] Ni X J, Wong Z J, Mrejen M, Wang Y and Zhang X 2015 *Science* **349** 1310

[11] Zheng B, Zhu R R, Jing L Q, Yang Y H, Shen L, Wang H P, Wang Z J, Zhang X M, Liu X, Li E P and Chen H S 2018 *Adv. Sci.* **5** 1800056

[12] Zhang X W, He X and Wu L Z 2019 *Chin. Phys. B* **28** 064403

[13] Zhang R Y, Zhao Q and Ge L M 2016 *Chin. Phys. B* **25** 084702

[14] Diatta A and Guenneau S 2016 *J. Phys. D: Appl. Phys.* **49** 445101

[15] Molina-Valdovinos S, Lamas-Martínez K J, Briones-Torres J A and Rodríguez-Vargas I 2022 *J. Phys.: Condens. Matter* **34** 195301

[16] Wu Q, Zhang K, Meng F Y and Li L W 2008 *J. Phys. D: Appl. Phys.* **42** 035408

[17] Wang X H, Qu S B, Xia S, Wang B K, Xu Z, Ma H, Wang J F, Gu C, Wu X, Lu L and Zhou H 2010 *Chin. Phys. B* **19** 064102

[18] Zhan J, Li K, Zhou Y, Liu X L and Ma Y G 2021 *ACS Appl. Mater. Inter.* **13** 17104

[19] Lai Y, Chen H Y, Zhang Z Q and Chan C T 2009 *Phys. Rev. Lett.* **102** 093901

[20] Yang C F, Yang J J, Huang M, Xiao Z and Peng J H 2011 *Opt. Express* **19** 1147

[21] Yan S, Wang T, Li T and Liang C H 2015 *IEEE Antenn. Wirel. Propag.* **14** 1550

[22] Rajput A and Srivastava K V 2017 *IET Microw. Antenn. Propag.* **11** 1051

[23] Guenneau S, Lombard B and Bellis C 2021 *Appl. Phys. Lett.* **118** 191102

[24] Yang C F, Huang M, Yang J J, Feng W J, Mao F C and Li T H 2019 *OSA Continuum* **2** 1259

[25] Lai Y, Ng J, Chen H Y, Han D Z, Xiao J J, Zhang Z Q and Chan C T 2009 *Phys. Rev. Lett.* **102** 253902

[26] Xu Y D, Gao L and Chen H Y 2011 *Front. Phys. China* **6** 61

[27] Li Z, Zang X F, Cai B, Shi C and Zhu Y M 2013 *Opt. Commun.* **308** 95

[28] Mei J S, Wu Q, Zhang K, He X J and Wang Y 2016 *Opt. Commun.* **368** 113

[29] Chen T, Zheng B and Yang Y 2019 *Light-Sci. Appl.* **8** 1

[30] Yang C F, Huang M, Yang J J, Mao F C and Li T H 2018 *Opt. Express* **26** 24280

[31] Yang C F, Huang M, Li T H, Yang J J, Mao F C and Xue Y Y 2019 *AIP Adv.* **9** 025028

[32] Li J S and Pendry J B 2008 *Phys. Rev. Lett.* **101** 203901

[33] Silva D G, Teixeira P A, Gabrielli L H, Junqueira M A and Spadoti D H 2017 *Opt. Express* **25** 23517

[34] Han T C, Tang X H and Xiao F 2010 *IEEE Microw. Wirel. Co.* **20** 64

[35] Han T C, Qiu C W and Tang X 2010 *Opt. Lett.* **35** 2642

[36] Zheng B, Madni H A, Hao R, Zhang X M, Liu X, Li E and Chen H S 2016 *Light-Sci. Appl.* **5** e16177

[37] Chen T H, Zheng B, Yang Y H, Shen L, Wang Z J, Gao F, Li E P, Luo Y, Cui T J and Chen H S 2019 *Light-Sci. Appl.* **8** 1

[38] Yang J J, Huang M, Yang C F and Yu J 2011 *Eur. Phys. J. D* **61** 731

[39] Rajput A and Srivastava K V 2017 *Plasmonics* **12** 771

[40] Xuan Y and Xu X 2019 *J. Microw. Opt. Electr. Appl.* **18** 184

[41] Huang T Y, Lin J H, Lee T and Yen T J 2019 *J. Opt.* **21** 08LT01